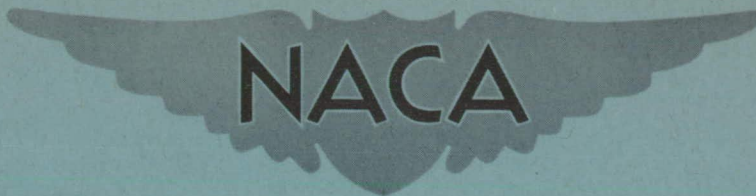


RELEASE DATE MAY 10 1949

RM No. E9C17

naca/8

NACA RM No. E9C17



RESEARCH MEMORANDUM

AN ELECTRIC THRUST METER SUITABLE FOR FLIGHT

INVESTIGATION OF PROPELLERS

By Porter J. Perkins, Jr. and Morton B. Millenson

Lewis Flight Propulsion Laboratory
Cleveland, Ohio

REVIEWED BUT NOT
EDITED

NATIONAL ADVISORY COMMITTEE
FOR AERONAUTICS

WASHINGTON
May 9, 1949

FILE COPY
To be returned to
the files of the National
Advisory Committee
for Aeronautics
Washington, D. C.

B

NATIONAL ADVISORY COMMITTEE FOR AERONAUTICS

RESEARCH MEMORANDUM

AN ELECTRIC THRUST METER SUITABLE FOR FLIGHT

INVESTIGATION OF PROPELLERS

By Porter J. Perkins, Jr. and Morton B. Millenson

SUMMARY

A lightweight instrument that utilizes resistance-wire electric strain gages to measure propeller-shaft thrust has been developed. A wind-tunnel investigation on a propeller installed on a single-engine pursuit airplane showed that the instrument gave a reliable indication of propeller-shaft thrust to an accuracy of ± 2 percent within its calibrated range. No attempt was made to determine the relation of indicated shaft thrust to net propeller thrust.

INTRODUCTION

Measurement of propeller thrust during icing conditions is essential to determine the aerodynamic effects of ice formations on propellers or to evaluate the effectiveness of ice-protection methods. An investigation in the 16-foot tunnel at the NACA Langley laboratory showed no serious effects on propeller performance of an artificial simulation of ice on the blades (reference 1). An exact measure of the effect of the propeller alone can be obtained from propeller thrust measurements with and without ice protection during icing conditions. Other conditions being equal, the net change in thrust caused by ice formations is indicated by a change in propeller-shaft thrust.

An investigation of propeller-icing effects and various systems of thermal ice protection has been made under simulated icing conditions in the icing research tunnel at the NACA Lewis laboratory. The need for an accurate device to measure propeller thrust and especially to measure incremental changes in thrust due to ice formations, when other conditions remain constant, led to the construction of a thrust meter of an electric strain-gage type to be installed on the propeller shaft; the thrust meter utilizes an electric circuit similar to that of the NACA electric torque meter described in reference 2.

The object of the development was to provide a rugged and reliable lightweight instrument protected from icing conditions, unaffected by temperature or humidity changes, and capable of measuring propeller-shaft thrust or incremental thrust changes to the accuracy required. The thrust meter that was developed can simultaneously indicate and record to an accuracy of ± 2 percent. Considerable experimental use has established the ruggedness of the load-pickup device. Comparisons of calibrations made over a period of several months during which the pickup was mounted in different nose gear boxes indicate inherent stability of the entire unit. Ready adaptability of the design to various propeller shafts and ease of changing the power-supply unit for operation on available airplane power permits use of this meter in both wind-tunnel and flight investigations. The construction and several means of calibrating the device as well as results obtained with it on a single-engine pursuit airplane in the icing research tunnel are reported.

THRUST METER

The NACA electric thrust meter consists of two principal units: a mechanical lever system to transfer propeller-shaft axial loads from the main thrust bearing to strain-sensitive electric gages; and an electric circuit, containing an indicator or recorder that may be calibrated in pounds thrust, to measure the resulting effect on the gage elements.

Details of the thrust-meter installation in the nose gear case of a single-engine pursuit airplane sectioned at a typical load-transfer location are shown in figure 1. Photographs of the mechanical parts of the thrust meter before assembly, after assembly, and a close-up of the assembly at a typical load-transfer location are shown in figure 2. A close-up view of the nose of the airplane with thrust meter installed on the reduction-gear case is shown in figure 3.

The operation of the mechanical system is illustrated in figure 1. The propeller shaft transmits an axial load through the outer race of the main thrust bearing A to a floating load-transfer ring B. The load-transfer ring contains four equally spaced axial projections, which transfer the load to matching radial cantilever members on a thrust-pickup ring C bolted to the reduction-gear case behind the propeller-pitch-control brush holder D. Relative rotation between the thrust-pickup ring and the load-transfer ring, caused by slow rotation of the thrust-bearing outer race, is prevented by two loose-fitting dowel pins.

Strain gages E, similar to those described in reference 3, are cemented to each side of the radial members so that propeller thrust loads apply compression to the forward gage and tension to the rear gage. Gages are needed only on two opposite members of the pickup ring but, in actual practice, a complete set of eight gages is so installed and calibrated that a spare circuit is available if desired.

The load-transfer and thrust-pickup rings are designed to displace the thrust bearing to the rear of its normal position in order that the bearing will be restrained only by the thrust-pickup system in the positive thrust direction. The thrust-bearing displacement and an initial deflection force on the strain gages is accomplished by first inserting a 0.012-inch spacer F between the bearing rear-retainer ring G and the gear case H and then selecting an appropriate thickness of incompressible (copper) gaskets I and J and steel spacer K to replace the fiber gasket normally installed against the gear case. An axial force of about 100 pounds has been found desirable to insure good contact for all thrust members.

Sufficient space for the thrust meter was obtained in this installation by machining 0.125 inch from the rear face of the propeller-pitch-control brush holder, by inserting a 0.125-inch spacer L behind the rear cone M to move the propeller forward, and by substituting a thinner cover plate and oil-retainer assembly N for the standard assembly. The standard fiber gasket O is used with the thin cover plate. The rigidity of the thrust-pickup ring and brush holder combine to reduce elastic deformation other than in the radial gage members. A thrust-bearing clearance P of approximately 0.010 inch is adequate for full range.

Details of the electric circuit of the thrust meter and curves showing its calibration are given in the appendix.

OPERATION

An investigation was conducted with the thrust meter to determine its capacity for indicating the variation with the advance-diameter ratio (V/nD) (V , tunnel air velocity; n , propeller rotational speed; and D , diameter of propeller) of the indicated shaft thrust coefficient C_T for a four-blade propeller with a diameter of 10.2 feet. No attempt was made to determine the relation of indicated shaft thrust to net propeller thrust. Measurements were made of the thrust of the normal propeller with four

smooth blades and with the propeller having added drag that might be similar to that caused by ice. The drag was introduced by two full-length spoilers mounted on both faces of two opposite blades of the four-blade propeller.

A blade setting of 25° at 75 percent of the propeller radius was held constant during this investigation. The V/nD range was obtained by varying both V and n . Tunnel airspeed was taken as that obtained by tunnel calibration at 75 percent of the propeller radius. The accuracy of the airspeed measurements was estimated to be within ± 2 percent. Propeller speed was measured by a chronometric tachometer with an accuracy of ± 0.5 percent.

RESULTS AND DISCUSSION

The curves presented in figure 4 show the change of thrust coefficient resulting from two types of full-length spoiler mounted on both faces of two opposite blades of the four-blade propeller as compared with the performance of a propeller with four smooth blades. These data indicate that the precision of the shaft-type thrust meter should be adequate for the measurement of incremental changes in propeller performance due to serious ice formations or due to the refreezing of melted water behind a heated leading edge.

During the investigation in the tunnel, the pickup unit of the thrust meter was affected by axial vibration of the propeller shaft at very low thrust values. This vibrational force added to the thrust force, resulting in higher thrust indications. A study of figure 1 shows that these high readings can be expected if the axial vibratory displacement of the shaft is greater than the displacement due to thrust alone. The forward amplitude of the vibratory cycle will, in net effect, increase the total displacement of the thrust bearing from its zero position against the rear-retainer ring because the rearward amplitude is limited by the fixed rear-retainer ring. The resistance in series with the microammeter together with its own internal damping prevents the meter from following the vibratory effect on the circuit. This mode of vibration is believed to be peculiar to the tunnel installation for one propeller configuration at low thrust values and would not, in general, affect the operation of the instrument.

Extensive use of the thrust meter at tunnel-air temperatures from 0° to 100° F, in simulated rain and severe icing conditions, discloses no inherent operational difficulties with the instrument.

Errors due to zero-drift residual friction or gage-temperature variation from starting to running conditions can be eliminated by a simple procedure. The instrument is allowed to warm up for about 20 minutes before reading the initial zero and starting the propeller. The zero reading is again taken immediately after stopping the propeller. If the initial zero differs from the final value, which may be the case if vibration eliminates residual friction, the final value is used and subtracted from all meter readings obtained during that run. The shaft thrust is then obtained from the calibration curve using the corrected net meter reading.

CONCLUSIONS

Results of a tunnel investigation of the electric propeller-shaft thrust meter installed on a single-engine pursuit airplane show that the meter reliably indicates propeller-shaft thrust with an accuracy of ± 2 percent within its calibrated range. Measurement of propeller-shaft thrust with this type of instrument is useful in determining for a given installation the relative effects on thrust of various blade-surface-roughness conditions resulting from ice formations.

Lewis Flight Propulsion Laboratory,
National Advisory Committee for Aeronautics,
Cleveland, Ohio.

APPENDIX - ELECTRIC CIRCUIT AND CALIBRATION

OF THRUST METER

Electric Circuit

The four strain gages on opposite radial members are electrically connected to form a Wheatstone bridge. A regulated direct-current voltage is impressed on two opposite corners of the bridge and a microammeter connected across the other two corners to measure the bridge unbalance. A high-resistance shunt is placed in parallel with one bridge arm to bring the bridge into balance at zero thrust. Whenever a thrust load is applied to the radial members, strain occurs in the gages, changes their resistance, unbalances the bridge, and causes current to flow through the meter circuit. Within the limits of strain for which Hooke's law applies, the meter current is proportional to the thrust load. Temperature changes are self-compensating in the bridge circuit within the over-all accuracy of the thrust meter because all the gages are subject to the same temperature conditions.

A schematic diagram of the power supply and bridge circuit is shown in figure 5. Values shown for the various elements are typical and can be varied to meet the requirements of a particular installation.

In the installation in the icing research tunnel, a common power source was used for both the thrust meter and for an NACA electric torquemeter of the type described in reference 2. This power source and certain external parts of both meter circuits are assembled in a single chassis, as shown in figure 6. A 120-volt alternating-current supply is connected through a double-pole switch S_1 and protected by fuses F_1 . (See fig. 5.) This power is transformed to 240 volts and rectified by a bridge-type dry-disk rectifier B, which has an output of approximately 150 volts direct current. A condenser C is connected across the rectified output to smooth out the voltage pulsations. Power from the rectifier is split into two parallel meter circuits which, with the exception of the common direct-current source, are independent of each other.

The direct current for the thrust meter passes through a current-regulating resistor R_1 and three iron-filament ballast tubes T, which regulate the current at about 250 milliamperes. A single ballast tube with appropriate characteristics would be

adequate. The value of resistor R_1 is adjusted to enable the ballast tubes to operate in the flat portion of the calibration curve. A shunt resistor R_2 limits the voltage drop across the bridge circuit to approximately 80 volts. A series resistor R_3 is also inserted in the bridge circuit to limit the current. The total power consumed by the thrust meter is approximately 40 watts.

The four strain gages G_1 , G_2 , G_3 , and G_4 are made with Advance wire of 0.0015-inch diameter and have an approximate resistance of 500 ohms. In this installation, the size of the cantilever members limits the gages to a length of $3/8$ inch and a width of $15/16$ inch. The gages are constructed and attached with phenol-formaldehyde cement according to the procedure given in reference 3. After wiring was complete, the gages, connections, and exposed wires were painted with a phenol-formaldehyde cement and baked to protect the circuit from water and oil.

The strain-gage bridge is brought to balance at zero load by means of the shunt resistor R_4 connected across one of the gages but located in the power-supply chassis. In order to preserve the temperature-compensating properties of the circuit, the strain gages used should be so nearly alike that the value of resistor R_4 is more than 25,000 ohms. A switch in this shunt, which when opened will unbalance the bridge, would provide a means of checking the operation of the circuit under no-load conditions.

The bridge unbalance can be measured with a low-period microammeter or with a recording galvanometer; or the unbalance can be simultaneously indicated and recorded with a combination of microammeter and self-balancing recording potentiometer, as indicated in figure 5. In this installation, a high-precision low-resistance microammeter with a range of 0 to 50 microamperes gave nearly full-scale readings for a shaft thrust of approximately 2000 pounds with a meter-circuit total resistance of 1900 ohms, which consisted of the resistances of the microammeter M , sensitivity-control resistors R_5 and R_6 , and fuse F_2 . The recording potentiometer was connected across shunt resistor R_6 and the meter circuit was protected by the 2-milliamperere fuse and switch S_2 . In an earlier installation, a microammeter with a range of only 0 to 20 microamperes was used with either of two sensitivity-control resistors. These resistors could be selected with a switch and they provided total meter-circuit resistances of 2000 and 4600 ohms to give approximately full-scale readings for thrusts of 1000 and

2000 pounds, respectively. The high accuracy and range of the self-balancing recording potentiometers eliminates the need for a dual sensitivity range in this installation.

Calibration

A dynamic calibration of the thrust meter was made with the propeller removed from the airplane by applying a known axial load to the propeller shaft, as shown in figure 7. The extension drive shaft of the airplane was first disconnected at the center bearing to permit free turning of the reduction-gear unit and propeller shaft. A 3-horsepower electric motor, fastened to the tunnel floor under the nose of the airplane and connected to the extension shaft above by a flat belt, turned the propeller shaft approximately 700 rpm. This speed provided the normal operating oil pressure of 80 pounds per square inch in the reduction-gear case. Tension was applied to the shaft by means of a horizontal cable attached to a shaft nut containing a ball-bearing swivel. The meter readings plotted against applied shaft tension are shown in figure 8 for an installation having a meter circuit resistance of 4600 ohms.

A static calibration to check the dynamic calibration was made in a standard hydraulic testing machine. A compressive load was applied to the pickup and transfer rings placed between the jaws of the machine. The static-calibration curve (fig. 9) shows that the meter readings for decreasing loads are slightly higher than those for increasing loads. This effect is not noticeable in the dynamic-calibration curve (fig. 8). This hysteresis effect is probably caused by friction between the projection of the load-transfer ring and the radial members of the thrust-pickup ring as they deflect under nonvibratory loading conditions. The effects of the reduction-gear lubricating system and gear-contact vibrations during operation tend to eliminate most of the effect of friction between these two parts. A comparison of static and dynamic calibrations is shown with the static-calibration curve in figure 9.

When the pickup unit was installed and the propeller was mounted on the airplane, another static calibration was made to determine the effect of the static weight of the propeller on the previous dynamic calibration. A comparison of these calibrations is shown in figure 10. The characteristic hysteresis effect of the previous static calibration also appears in this static calibration. A straight line was drawn representing an average between

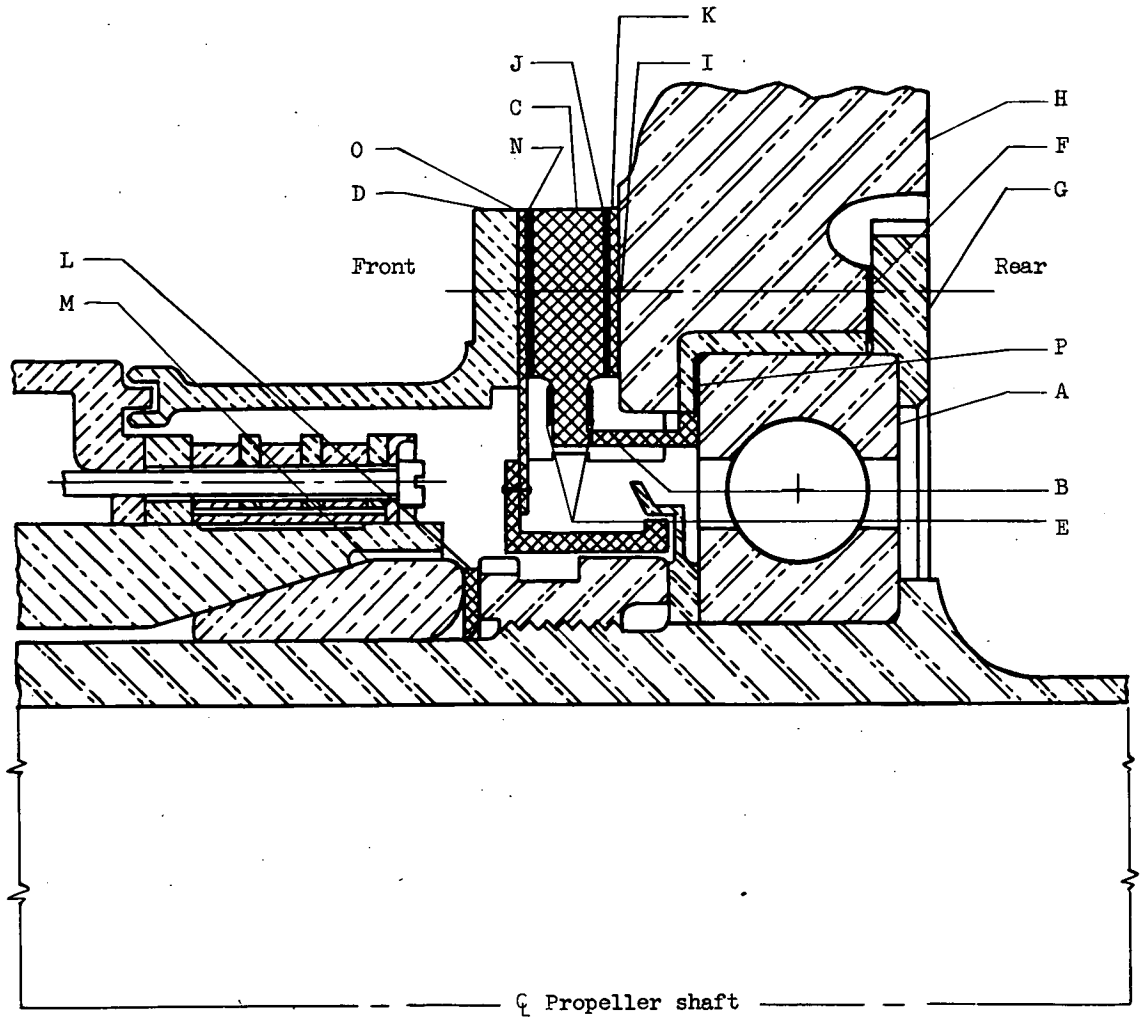
the plotted points. As a result of the static weight of the propeller, the slope of this line is slightly greater than that of the dynamic-calibration line. Over a period of approximately 10 months, two more dynamic calibrations without propeller indicated no noticeable change in the original dynamic-calibration curve of figure 8.


The thrust-meter calibration constant as determined by dynamic calibration was 111 pounds per microampere above a value of 100 pounds. Below this value the loads are inadequate to cause uniform deflection of the radial members on the pickup ring.


The sensitivity of the meter circuit with the original microammeter was adjusted by increasing the total resistance to 4600 ohms to give a reading of approximately 50 pounds per scale division, and thus permitted estimation to the nearest 25 pounds. In the revised circuit (fig. 5) with a meter circuit resistance of 1900 ohms and a microammeter of greater range, the sensitivity of the indicator was approximately the same. The sensitivity of the recording potentiometer was, however, greater for each chart division (0.05 in.) and corresponded to $16\frac{1}{2}$ pounds of thrust; interpolations to the nearest 5 pounds could be made with ease.


REFERENCES

1. Corson, Blake W., Jr., and Maynard, Julian D.: The Effect of Simulated Icing on Propeller Performance. NACA TN No. 1084, 1946.
2. Nettles, J. Cary, and Hanson, Morgan P.: Flight Tests of a P-63A-1 Airplane with an Electric Torquemeter. NACA ARR No. E5B16, 1945.
3. Nettles, J. Cary, and Tucker, Maurice: Construction of Wire Strain Gages for Engine Application. NACA ARR No. 3L03, 1943.



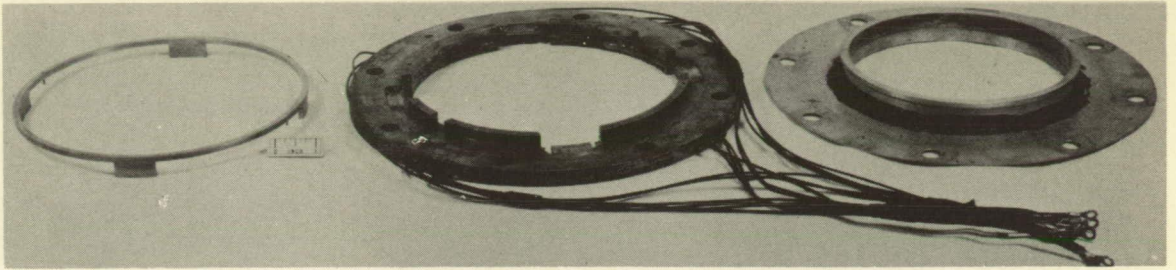

Propeller
assembly


Reduction-gear
assembly

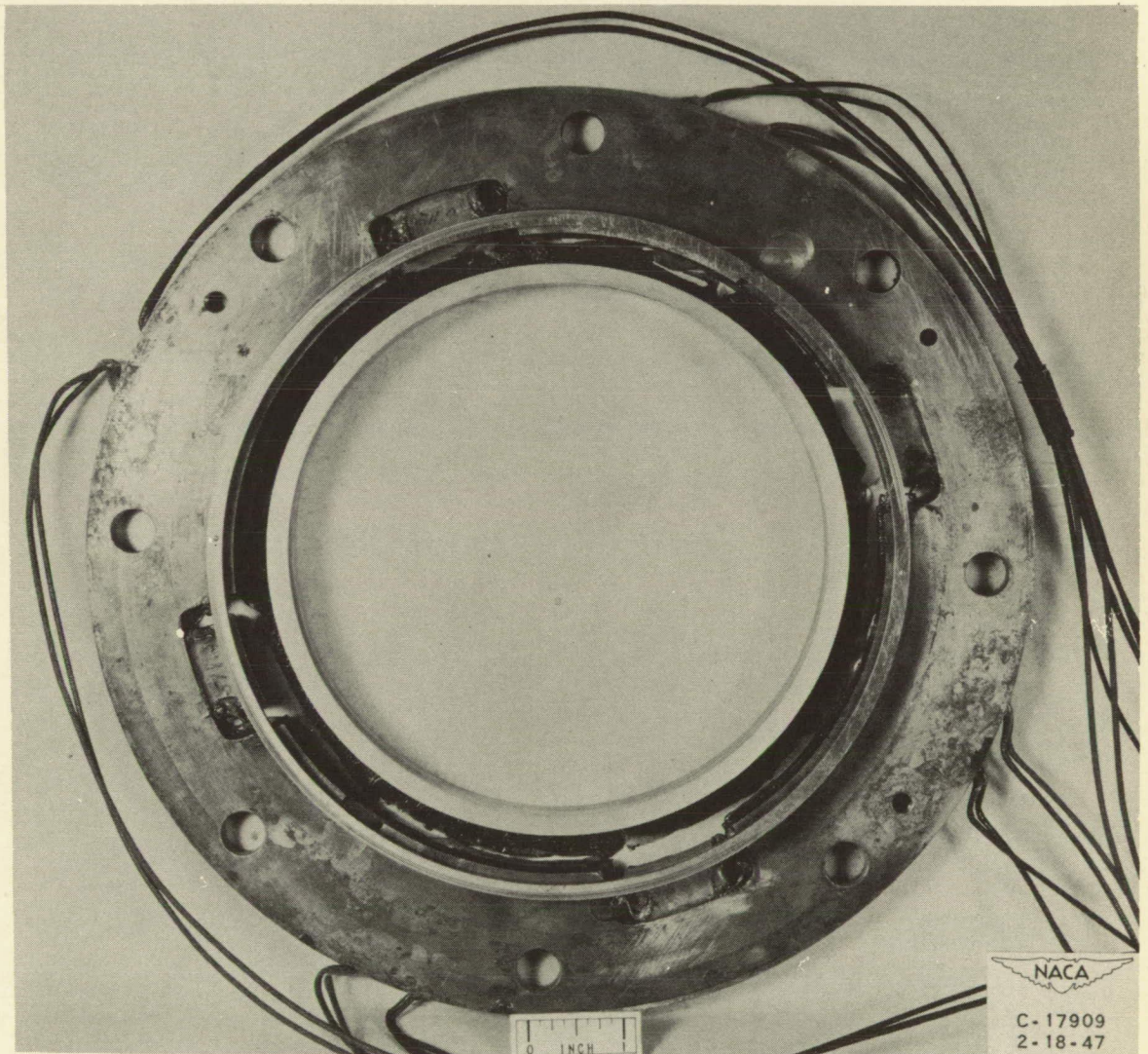

Thrust-meter
assembly

- | | |
|--|---|
| A Thrust bearing | J Front copper gasket, 0.010 in. |
| B Load-transfer ring | K Steel spacer, fitted |
| C Thrust-pickup ring | L Propeller-cone spacer, 0.125 in. |
| D Brush holder, 0.125 in. removed from rear face | M Rear propeller cone, standard |
| E Strain gages | N Front cover plate and oil-retainer assembly |
| F Rear clearance spacer, 0.012 in. | O Fiber gasket, standard |
| G Bearing rear-retainer ring, standard | P Bearing clearance, 0.010 in. for full range |
| H Reduction-gear case, standard | |
| I Rear copper gasket, 0.010 in. | |

Figure 1. - Section through nose of reduction-gear unit showing NACA electric thrust meter installed.



(a) From left to right, before assembly.

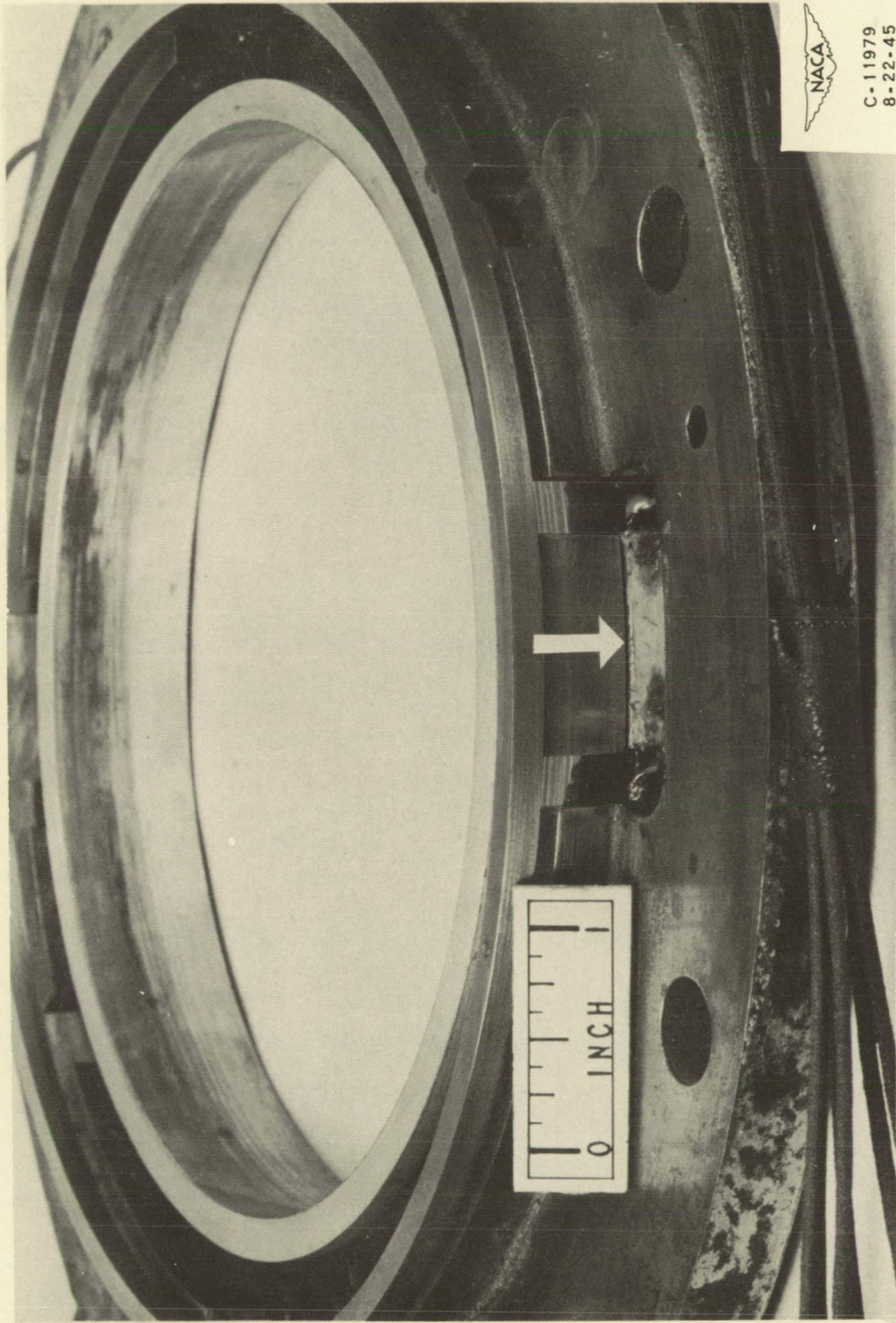


(b) From thrust-bearing (rear) side, after assembly.

Figure 2. - Views of load-transfer ring, thrust-pickup ring, and special cover plate.

Page intentionally left blank

Page intentionally left blank



(c) Close-up of assembly at typical load-transfer location.

Figure 2. - Concluded. Views of load-transfer ring, thrust-pickup ring, and special cover plate.

Page intentionally left blank

Page intentionally left blank

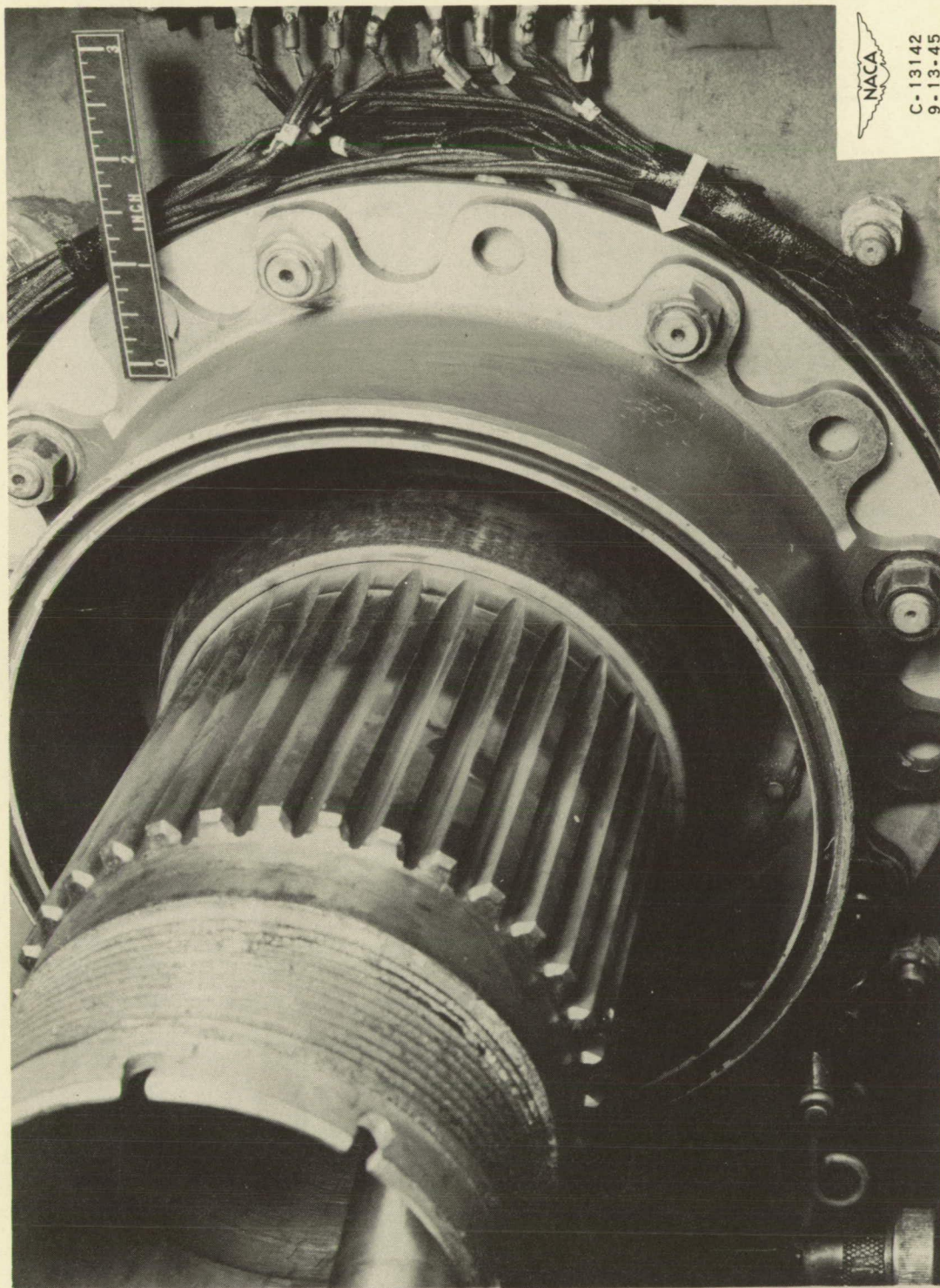


Figure 3. - Close-up view of airplane nose showing NACA electric thrust meter installed on reduction-gear case. Propeller removed.

Page intentionally left blank

Page intentionally left blank

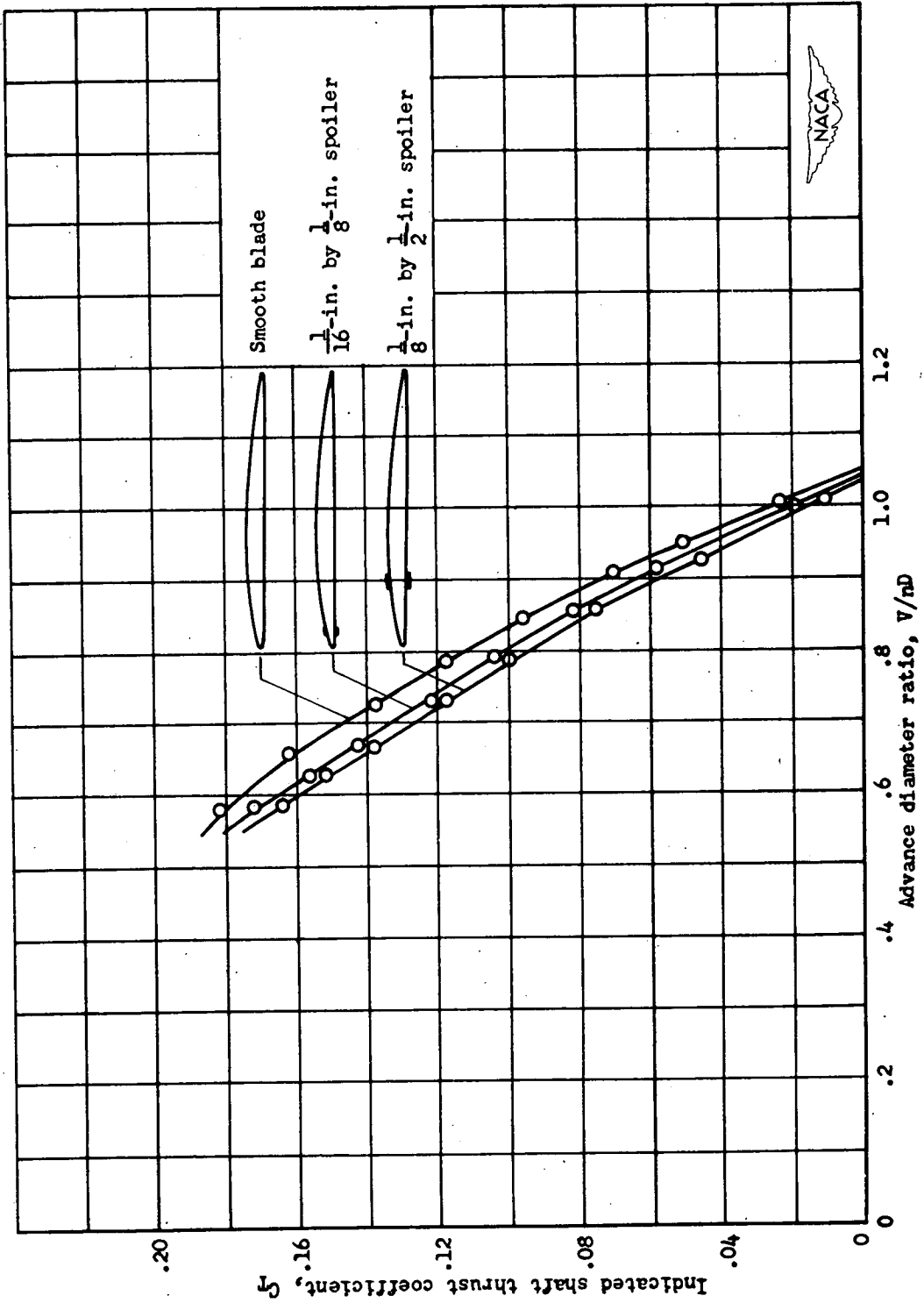
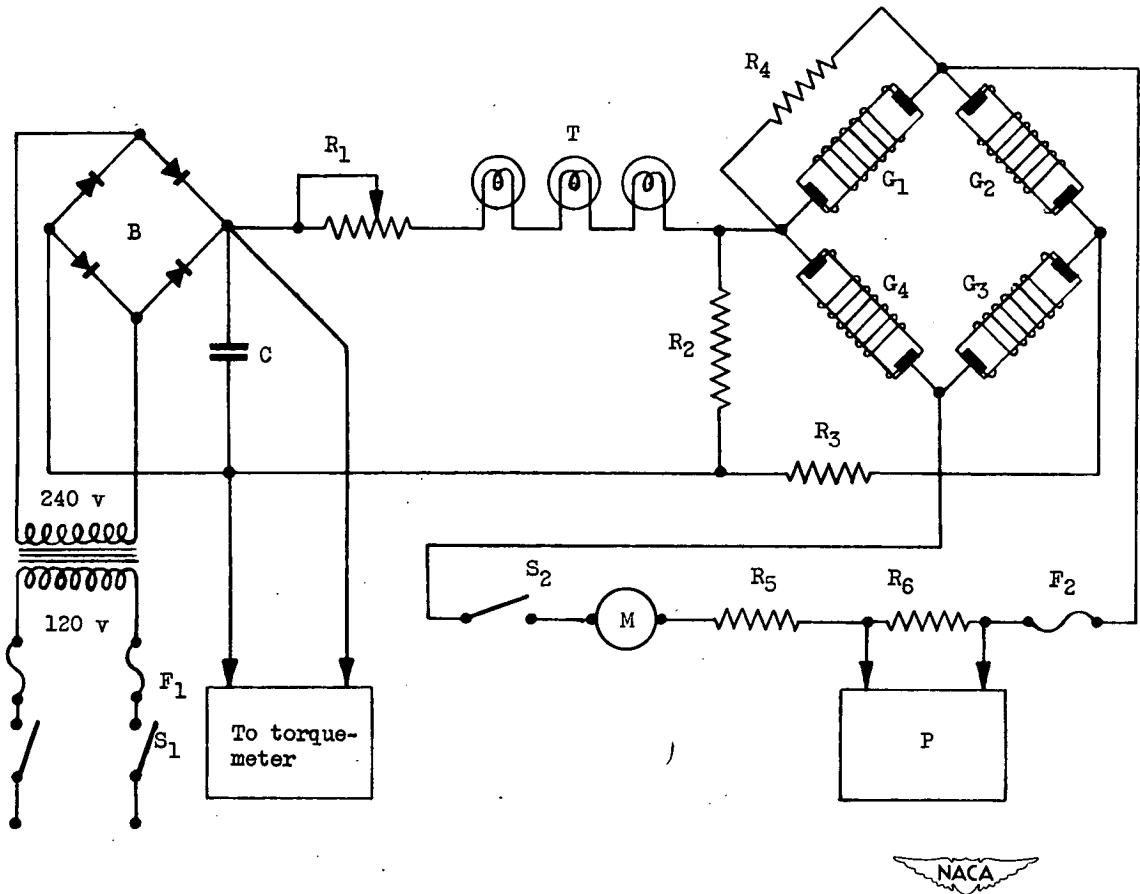


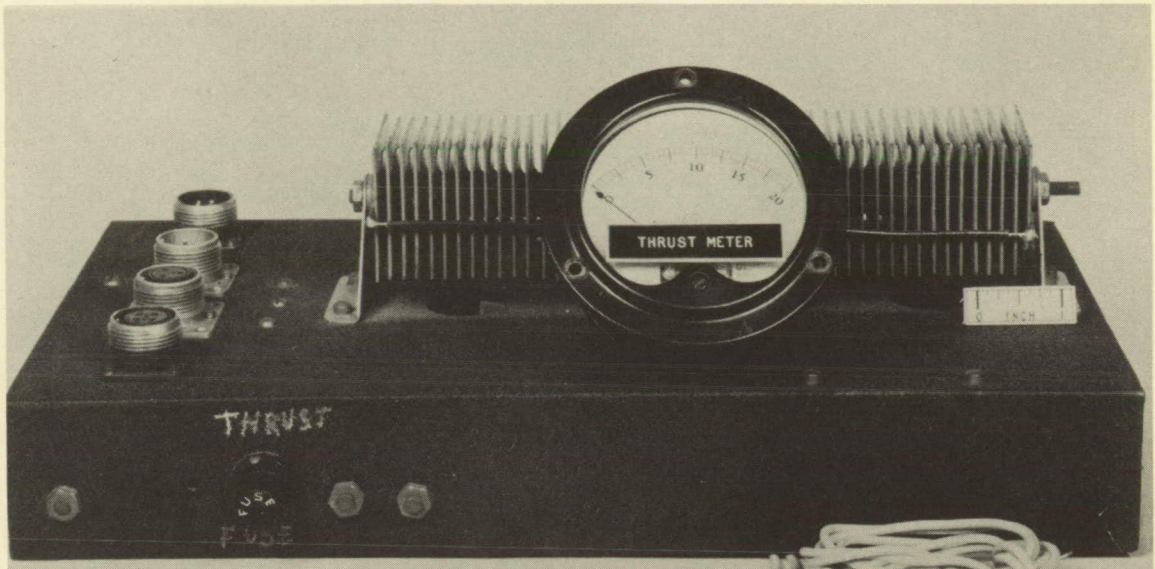
Figure 4. - Effect of propeller-blade surface spoilers on indicated shaft thrust coefficient as measured with NACA electric thrust meter.



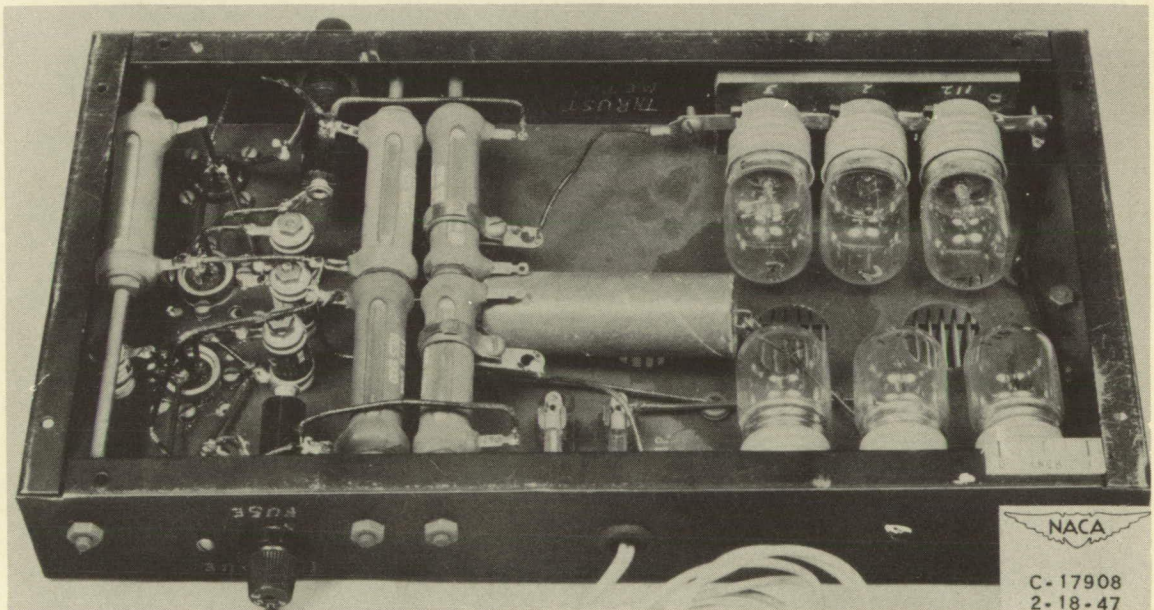
B Rectifier, bridge type dry disk
 C Condenser, 40 microfarads
 F₁ Fuses, 2 amperes
 F₂ Meter fuse, 100 ohms, 2 milliamperes
 G₁, G₂, G₃, G₄ Strain gages, 500 ohms each
 M Microammeter, 0-50 microamperes, 1200 ohms
 P Self-balancing recording potentiometer
 R₁ Current-regulating resistor, 500 ohms

R₂ Bridge-circuit shunt resistor, 1000 ohms
 R₃ Series resistor, 200 ohms
 R₄ Balancing shunt resistor, 29,575 ohms
 R₅ Sensitivity-control resistor, 400 ohms
 R₆ Sensitivity-control and potential-dropping resistor, 200 ohms (to suit recorder)
 S₁ Power switch, double pole
 S₂ Meter switch, single pole
 T Current-regulating ballast tubes

Figure 5. - Schematic wiring diagram of power source and circuit for NACA electric thrust meter.



(a) Meter as installed in panel board with engine control instruments.



(b) Under side of chassis showing arrangement of circuit parts.

Figure 6. - Power-supply chassis for NACA electric thrust meter and torquemeter and microammeter used with thrust meter.

Page intentionally left blank

Page intentionally left blank

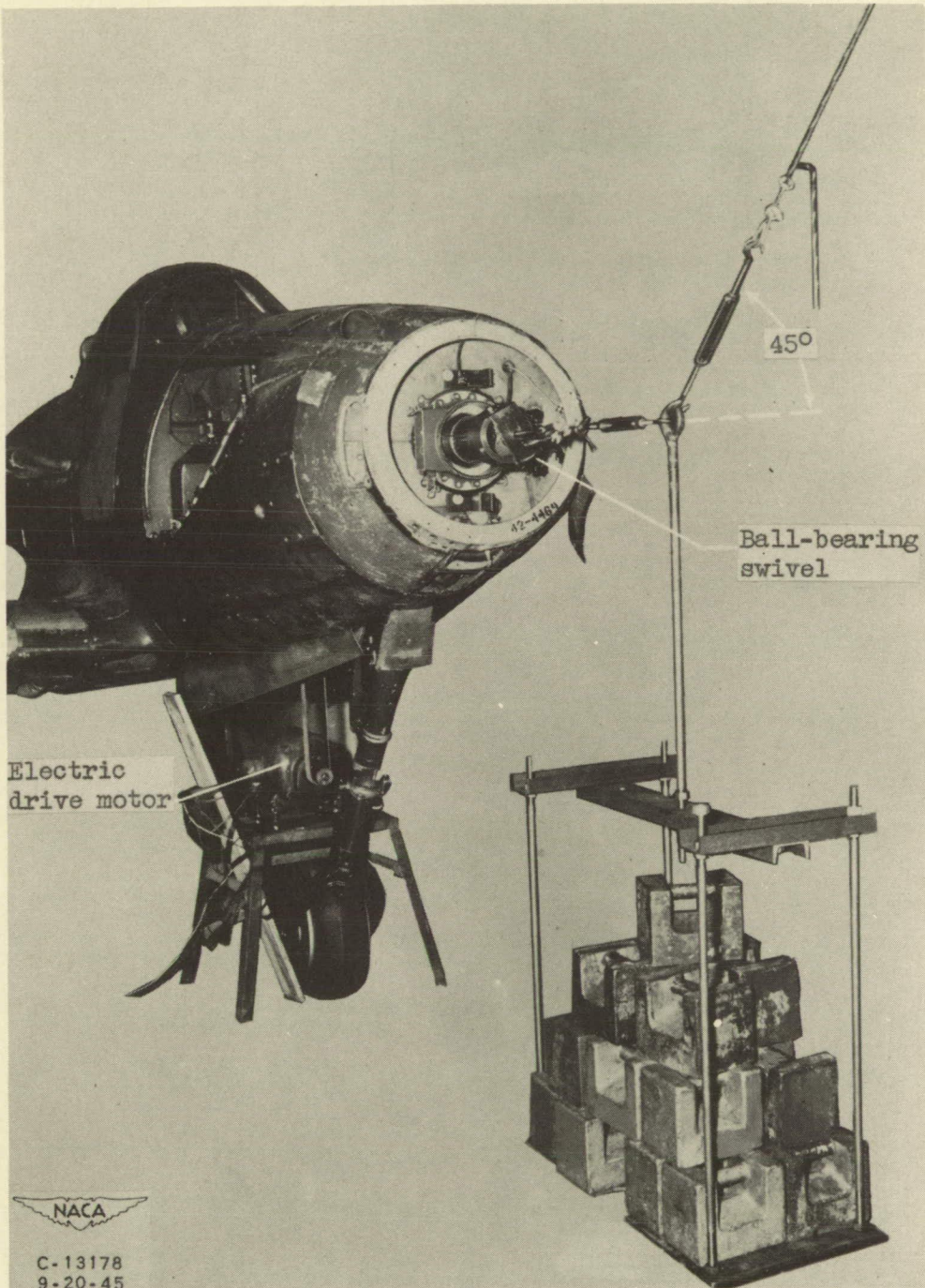


Figure 7. - Dynamic-calibration setup showing motor used for rotating shaft and method of applying load.

Page intentionally left blank

Page intentionally left blank

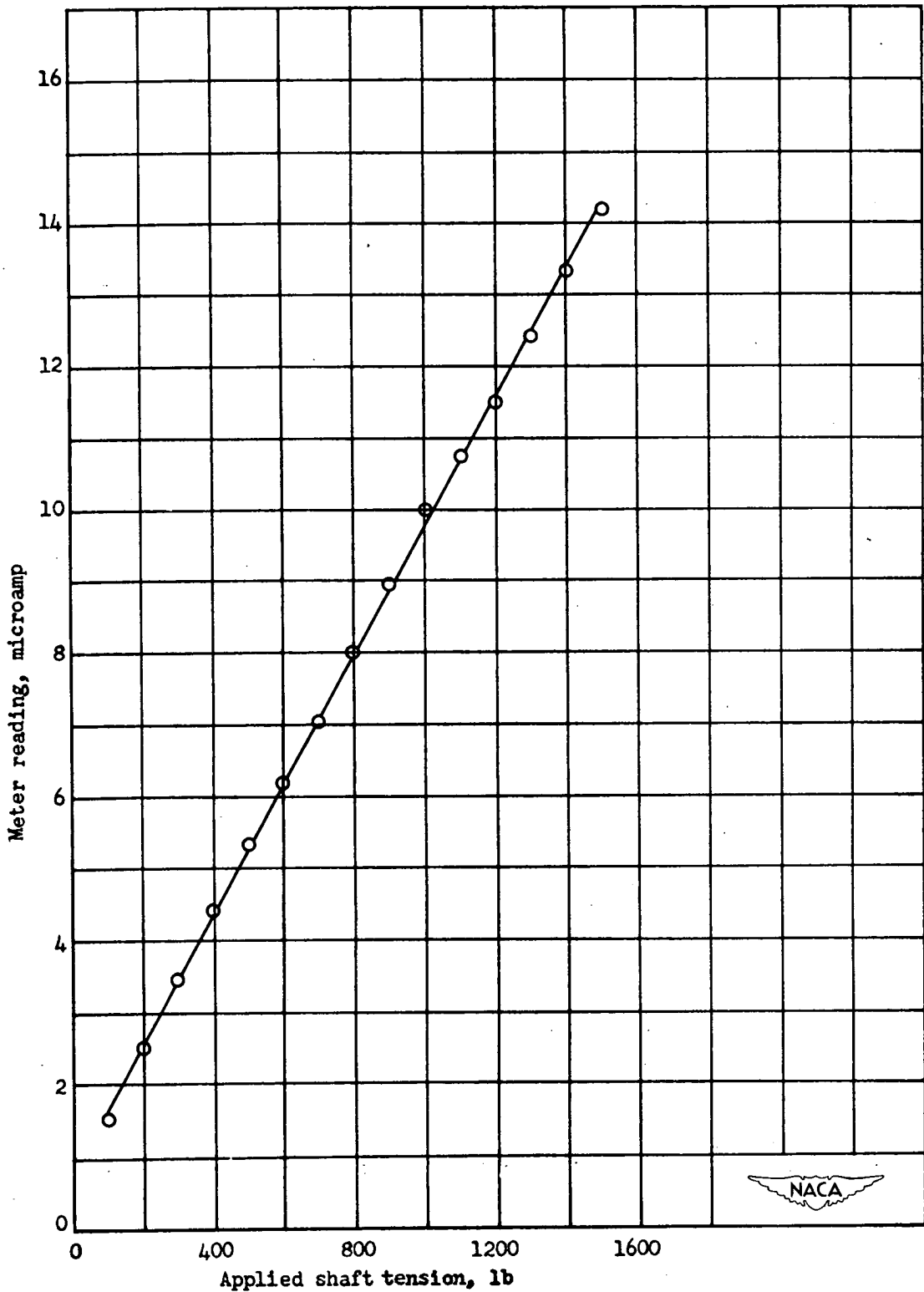


Figure 8. - Dynamic-calibration curve of NACA electric thrust meter.
Circuit resistance, 4600 ohms.

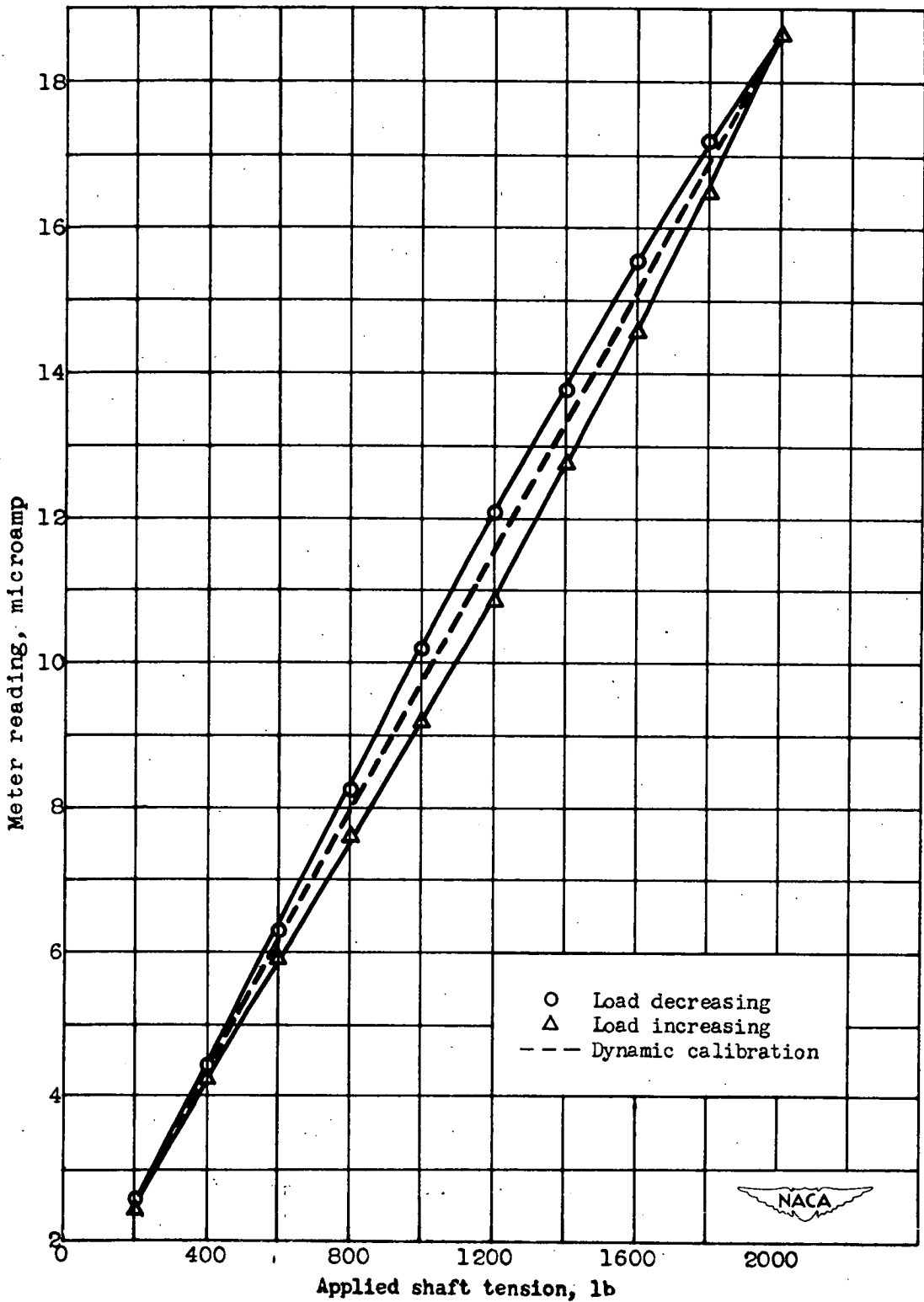


Figure 9. - Static calibration of thrust meter showing hysteresis as compared with dynamic calibration of NACA electric thrust meter.

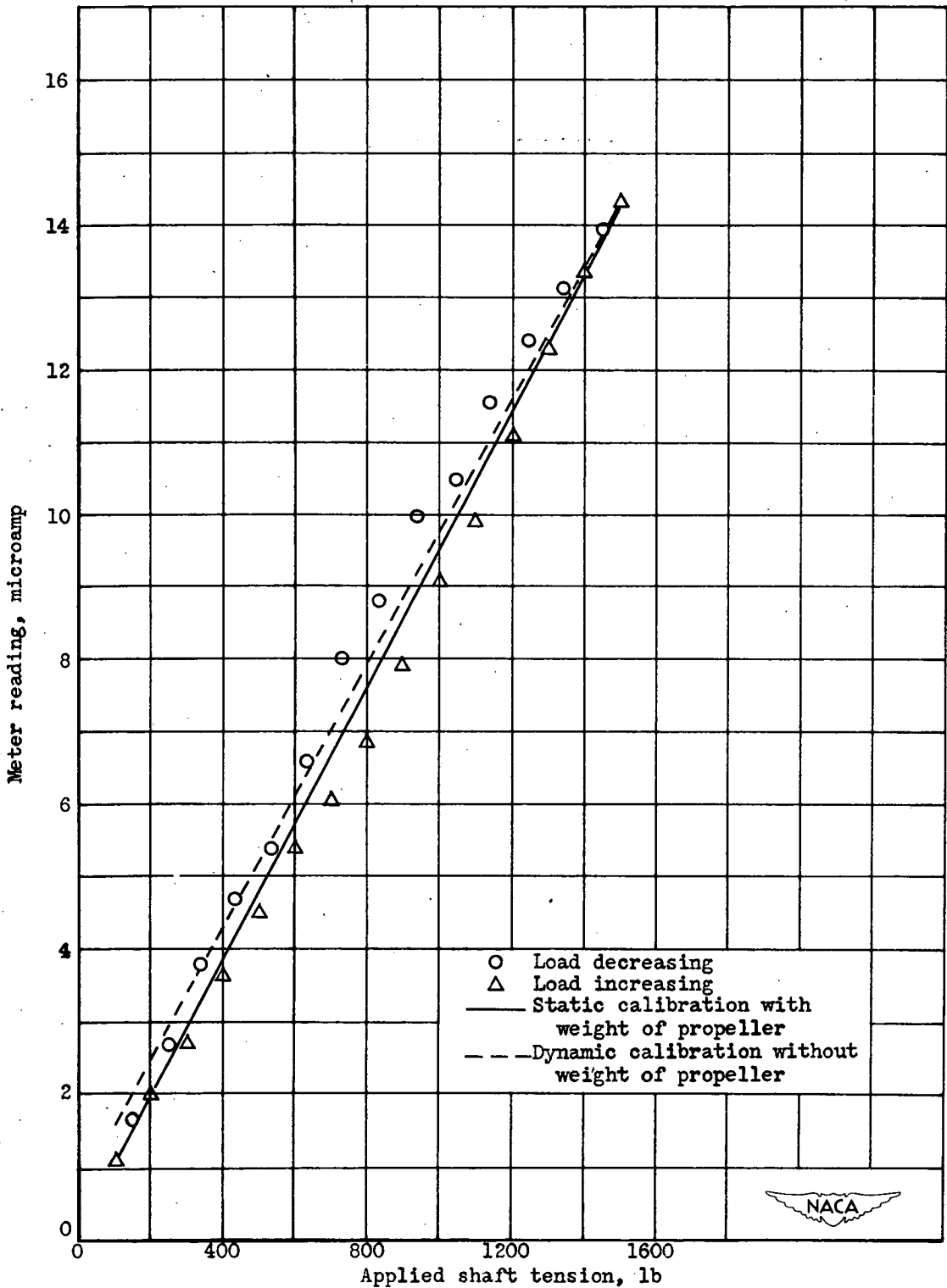


Figure 10. - Effect of static weight of propeller on calibration of NACA electric thrust meter.